Supplemental Material

Experimental protocols and analytical procedures

This section provides a brief description of the experimental protocols and analytical procedures of the studies included in this analysis. The characteristics of the subjects are reported in Table 1 of the main text.

Three-step hyperglycemic hyperinsulinemic clamp (3HGclamp)

The experimental procedures have been described in part previously (1). This analysis includes 7 of the 13 subjects participating in the original study; 6 subjects were excluded because of inconsistencies between insulin concentration, insulin secretion and insulin infusion data.

Experimental protocol

After an overnight fast, three consecutive 30-min square-wave steps of hyperglycemia were produced (on average 2.9, 5.8, and 10.6 mmol/L above baseline). Plasma glucose concentrations were maintained at the desired plateau by means of a variable 20% glucose infusion according to the glucose clamp technique (2). Each glucose infusion period was preceded by a priming glucose injection to reach the target glucose level faster. At time t = 90, an intravenous bolus of 5 g arginine followed, after 15 to 50 min, by a constant (24 pmol min^{-1} kg^{-1}) insulin infusion was given to raise glucose utilization to nearly maximal levels.

Three blood samples were taken during the basal period. Thereafter, blood samples were collected every 2 min for the first 10 min and every 5 min for the other 20 min of each step of the clamp. After the arginine bolus, blood was sampled every 2 min for 10 min. During insulin infusion, blood was sampled every 10 min.

Analytical procedures

Insulin and C-peptide were assayed in plasma by radioimmunoassay (Human Insulin-specific RIA kit from Linco Research, St. Charles, MO).

Hyperglycemic hyperinsulinemic clamp (HGclamp)

The experimental procedures have been described in detail previously (3).

Experimental protocol

Participants arrived at the metabolic ward at 8:00 hours after an overnight fast. After baseline blood sampling at time −30 min, saline was infused throughout the study until time 130 min. After drawing two further blood samples (−10 and 0 min), a glucose bolus, calculated to rapidly increase the glucose concentration into the readily accessible glucose distribution volume (150 ml/kg), was delivered in 90 s, followed by a continuous glucose infusion adjusted to achieve and maintain plasma glucose levels of 7.0 mmol/L above fasting values for 120 min. Blood samples for hormone measurements were collected every 2 min for the first 10 min and every 20 min until 120 min. At 120 min, an arginine bolus (5 g in a 20% water solution) was injected, and blood was collected every 2 min for the next 10 min.

Analytical procedures

Plasma insulin and C-peptide were measured using an electrochemiluminescence immune assay method (Cobas E411; Roche, Rotkreuz, Switzerland).

Intravenous glucose infusion producing a plasma glucose ramp (RAMP)

The experimental procedures have been described in detail previously (4).

Experimental protocol

Subjects were admitted to the metabolic ward after an overnight fast. Starting at time 0, glucose (20% dextrose) was infused at a variable rate to create a quasilinear increase in plasma glucose concentrations to peak values of ~22 mmol/L (in NGT) and ~28 mmol/L (in T2D) over 3 h. Blood samples were drawn for plasma insulin and C-peptide determination before glucose infusion and every 20 min thereafter. T2D patients' oral medications (metformin, sulfonylureas, and sitagliptin) were withdrawn 24–48 h before each study.

Analytical procedures

Plasma insulin and C-peptide were measured by an electrochemiluminescence assay on a COBAS e411 (Roche, Indianapolis, IN).

Paired OGTT and isoglycemic intravenous glucose infusion (IIGI-OGTT)

The experimental procedures have been described in detail previously (5).

Experimental protocol

Two studies were carried out in each subject after an overnight fast at 1-week intervals. In the first study, subjects underwent a 3-h OGTT (75 g). In the second study (isoglycemic test), the plasma glucose profile was reproduced by a variable intravenous glucose (20% dextrose) infusion. In both studies, venous blood was sampled at -30, 0, 10, 20, 30, 40, 60, 90, 120, 150, and 180 min for plasma insulin and C-peptide measurements. In T2D patients, glucose-lowering pharmaceutical treatments were withheld 3 weeks before the studies.

Analytical procedures

Plasma insulin was measured in duplicate by radioimmunoassay using a kit for human insulin with negligible cross-reactivity with proinsulin and its split products (Linco Research, St. Louis, MO). C-peptide was measured by radio-immunoassay (Linco Research).

Paired mixed meal and isoglycemic intravenous glucose infusion (IIGI-MMTT)

The experimental procedures have been described in detail previously (6).

Experimental protocol

Two studies were carried out within 2-7 days in each subject after an overnight fast. The first study was a standardized mixed meal consisting of one egg, 50g of parmesan cheese, and 75g of an aqueous solution of dextrose (53% carbohydrate, 30% fat, 17% protein, 560 kcal). The second study was an isoglycemic intravenous glucose infusion: the plasma glucose profile of the mixed meal was reproduced by a variable intravenous glucose infusion. In both studies, venous blood was sampled at -30, 0, 10, 20, 30, 40, 60, 90, 120, 150, 180, 210, 240, 270, and 300 min for plasma insulin and C-peptide measurements. The meal was ingested at time 0 (in <10min). In T2D patients, antidiabetic treatment was suspended 4 weeks before the study.

Analytical procedures

Plasma insulin and C-peptide were measured by electro-chemiluminescence (on a COBASe411; Roche, Indianapolis, IN).

Two-step isoglycemic hyperinsulinemic clamp (2ISOclamp)

The experimental procedures have been described in detail previously (7).

Experimental protocol

Study participants were admitted to the unit in the morning, after an overnight fast. The study protocol consisted of three periods: basal (from -145 to 0 min), low-insulin infusion (at a rate of 120 pmol min^{-1} m^{-2}, from 0 to 100 min), and high-insulin infusion (1200 pmol min^{-1} m^{-2}, from 100 to 200 min). Each insulin infusion was primed with a bolus designed as fourfold the constant infusion rate for the first 4 min. During insulin infusion, plasma glucose concentration was measured every 10 min and maintained at basal values by means of a variable 20% glucose infusion according to the isoglycemic clamp technique (2).

Blood sampling for the assay of plasma insulin was more frequent (every 2–5 min) during the first 50 min of each of the three study periods and was spaced at 10- to 15-min intervals thereafter. During the basal period, four to five blood samples were taken for plasma insulin determination.

Analytical procedures

Insulin was assayed in plasma by RIA (Human Insulin-specific RIA kit from Linco Research, St. Charles, MO).

One- or two-step euglycemic hyperinsulinemic clamp (2EUclamp)

The experimental procedures have been described in detail previously (8).

Experimental protocol

No NGT or IGT subject was taking any medication known to affect glucose tolerance. T2D subjects taking sulfonylureas or metformin (35%) had their oral hypoglycemic agent discontinued 3 days before the study. No diabetic subject had received treatment with a thiazolidinedione or insulin.

Subjects received a primed-continuous insulin infusion for 120 min. Straight after, a subset of subjects received a second primed-continuous insulin infusion for further 120 min. Infusion rates were 120

pmol min^{-1} m^{-2} (*N*=41; subject count after exclusions, as described below), 240 pmol min^{-1} m^{-2} (*N*=178), 60 pmol min^{-1} m^{-2} followed by 240 pmol min^{-1} m^{-2} (*N*=37), or 240 pmol min^{-1} m^{-2} followed by 960 pmol min^{-1} m^{-2} (*N*=119). During the last 30 min of the basal equilibration period, plasma samples were taken at 5- to 10-min intervals for the determination of plasma insulin concentrations. During insulin infusion, plasma glucose concentration was measured every 5 min, and a variable infusion of 20% glucose was adjusted, based on the negative feedback principle, to maintain the plasma glucose concentration at each subject's fasting plasma glucose level with a coefficient of variation less than 5%. In the diabetic group, the plasma glucose concentration was allowed to decline to 5.6 mmol/L, at which level it was clamped. Plasma samples were collected every 5–10 min from 90 to 120 min for the determination of plasma insulin concentrations. Basal C-peptide concentration was measured in the individuals with insulin infusion rate equal to 240 pmol min^{-1} m^{-2}, or to 240 pmol min^{-1} m^{-2} followed by 960 pmol min^{-1} m^{-2}.

Analytical procedures

Plasma insulin and C-peptide concentrations were measured by RIA using specific kits (Linco Research, St. Louis, MO).

Euglycemic hyperinsulinemic clamp with paired OGTT (EUclamp)

The experimental procedures have been described in detail previously (9).

Experimental protocol

A 75-g OGTT was given in the morning after an overnight fast. During the OGTT period (0-120 min), plasma samples were taken at 30-min intervals for measurement of insulin and C-peptide.

A euglycemic hyperinsulinemic clamp was performed on a separate day within 1 month of the OGTT. In the morning after an overnight fast, a primed-continuous infusion of insulin at a rate of 240 pmol min^{-1} m^{-2} was given simultaneously with a variable 20% dextrose infusion adjusted every 5 min to maintain plasma glucose levels within 0.8 mmol/L (±15%) of the target glucose level (4.5-5.5 mmol/L). Plasma samples for the measurement of insulin and C-peptide were taken during the basal period (-20 and 0 min) and at the end of the clamp (80 and 120 min).

Analytical procedures

Participants were recruited from the local population at 19 centers in 14 countries; samples were transported on dry ice at prearranged intervals to a central laboratory. Serum insulin and C-peptide were measured by a specific time-resolved fluoroimmunoassay (AutoDELFIA Insulin kit; Wallac Oy, Turku, Finland).

Hyperglycemic hyperinsulinemic clamp, euglycemic hyperinsulinemic clamp and OGTT (HGclamp/EUclamp)

The experimental procedures have been described in detail previously (10,11).

Experimental protocol

Study participants with T2D were treated with lifestyle only, insulin only, metformin only, or metformin plus insulin. Metformin was discontinued 36 h prior to testing. Patients did not receive long- or intermediate-acting insulin for 24 h prior to testing. The last dose of short-acting insulin was given 6–8 h prior to testing. Participants classified as NGT or IGT were not taking any medications known to affect glucose metabolism.

After overnight fasting, participants underwent a 2-h OGTT (1.75 g/kg, maximum 75 g). Blood samples were obtained at -15, 0, 15, 30, 60, 90, and 120 min for the measurement of insulin and C-peptide.

A 2-h hyperglycemic clamp (~225 mg/dl) was performed either the day after the OGTT or on a separate visit within a 1–4-week period. Plasma glucose concentration was rapidly raised to 225 mg/dl with a bolus dextrose infusion and maintained at 225 mg/dl with a variable-rate infusion of 20% dextrose for 2 h. Three basal and 13 post-basal blood samples were obtained for the measurement of insulin and C-peptide.

On a separate visit, after an overnight fast, a 180-min hyperinsulinemic-euglycemic clamp was started with a constant infusion of insulin (480 $pmol \cdot min^{-1} \cdot m^{-2}$). Plasma glucose was clamped between 90 to 100 mg/dl. Steady-state insulin was calculated as the mean of 4 insulin concentrations every 10 minutes over the last 30 minutes of the clamp.

Analytical procedures

Plasma insulin and C-peptide were determined by commercially available radioimmunoassay (Linco/Millipore, St. Charles, Missouri).

Data exclusion

Subjects with inconsistent insulin clearance data from the euglycemic clamp and fasting conditions were excluded. Specifically, an empirical hepatic insulin fractional extraction estimate, E_h^{emp}, was derived assuming linearity of insulin kinetics and using the values of exogenous (aka peripheral) and endogenous insulin clearance ($ExIC^{emp}$ and EIC^{emp}, respectively):

$$E_h^{emp} = 1 - \frac{ExIC^{emp}}{EIC^{emp}},$$

$$ExIC^{emp} = \frac{inf_{ss}}{ins_{ss} - ins_{bas}},$$

$$EIC^{emp} = \frac{ISR_{bas}}{ins_{bas}},$$

where inf_{ss} is the steady state intravenous insulin infusion rate during the euglycemic hyperinsulinemic clamp, ins_{ss} is the steady state plasma insulin concentration, ins_{bas} is basal insulin, and ISR_{bas} is the basal insulin secretion rate, computed from basal C-peptide concentration using the Van Cauter's model of C-peptide clearance (12). Subjects were excluded from the analysis if E_h^{emp} was less than -0.5 or greater than 1 at any insulin infusion level: 99 individuals were excluded from the 2EUclamp study, 43 from the EUclamp study, and none from the HGclamp/EUclamp study.

A few more exclusions were applied when any of the data required by the analysis was not available.

The mathematical model of insulin kinetics

The circulatory model.

The circulatory model of insulin kinetics included four interconnected blocks, each representing a group of organs: the chambers of heart and lungs (HL), the gut (GUT), the liver (LI) and the other organs (OO) (Figure S9; previous supplemental figures, S1 to S8, are introduced in the main text). In

a circulatory model, each block lumping various organs is regarded as a single inlet-single outlet organ and can be described mathematically by an impulse response (13). The organ impulse response is defined as the mass (in our case insulin) efflux observed at the outlet after a bolus injection of a unit dose into the inlet (with no insulin recirculation). After bolus injection into a peripheral vein, the insulin disappearance curve is the result of the combination of the impulse responses of the four interconnected blocks.

The impulse responses of the gut and the heart-lung block were assumed to be known and time-invariant. They were represented by two-exponential functions starting from zero and returning to zero after rising to an early peak, with integral equal to 1, as insulin fractional extraction was assumed to be negligible. This assumption implies that the impulse response coincides with the transit time density function of the organ block. Impulse responses were parameterized with the constants α and β (with α > β):

$$r(t) = \frac{\alpha\beta}{\alpha-\beta} exp^{-\beta t} - \frac{\alpha\beta}{\alpha-\beta} exp^{-\alpha t}.$$

The mean transit time (MTT) of r(t) was

$$MTT = \frac{1}{\alpha} + \frac{1}{\beta},$$

and the time of the maximum (t_M) was

$$t_M = \frac{ln(\alpha)-ln(\beta)}{\alpha-\beta}.$$

The values for α and β were derived from the values of MTT and t_M (see below). The transit time density functions of the LI and the OO blocks were represented in an analogous way, but including insulin extraction. The impulse responses were represented as (1-E(t))·r(t), where E(t) is the insulin fractional extraction from the considered block, with values between 0 and 1, and r(t) is the transit time density function, as represented above (14). E(t) was assumed to be a constant to be estimated for the OO block (extrahepatic extraction, E_{eh}), and a function of insulin concentration for the liver (hepatic extraction, $E_h(t)$, described in a specific section below).

The cardiac output F is the flow through the HL block; the portal vein and gut flow (F_{pv}) was assumed to be 20% of F (15); the liver flow (F_{li}) was calculated as the sum of the portal vein flow and the hepatic artery flow (F_{ha}, assumed to be 6% of F (15)); the difference between F and the liver flow represented the flow through the OO block (F_{oo}). F was assumed to remain constant during each test and equal to 3.2 L/min per m^2 of body surface area (7), multiplied by the plasma fraction of whole blood (1-H, where H=0.44 is the hematocrit) to obtain the actual insulin mass flux from the measurement of insulin concentration in plasma. Organ flows are summarized in Table S7 (previous supplemental tables, S1 to S6, are introduced in the main text).

For each block, MTT was derived as the ratio between its volume of distribution and the plasma flow perfusing the related organs. Volumes of distribution and their calculation are reported in Table S7. t_M was empirically assumed to be 0.05 min for the HL block and 0.1 min for the other blocks.

The derived values for α were 47.71, 24.51, 24.96 and 41.49 min^{-1} for the HL, GUT, LI and OO, respectively. The derived values for β were 5.90, 2.79, 2.69 and 0.70 min^{-1} for the HL, GUT, LI and OO, respectively.

Each block could be described via a state space representation:

$$\dot{X}(t) = AX(t) + Bu(t)$$

$$y(t) = CX(t)$$

$$A = \begin{bmatrix} -\alpha & 0 \\ \beta & -\beta \end{bmatrix}$$

$$B = (1 - E(t)) \begin{bmatrix} \alpha \\ 0 \end{bmatrix}$$

$$C = [0 \quad 1],$$

where the state X(t) is a column vector with two elements, u(t) and y(t) are input and output insulin fluxes, respectively, expressed as $pmol \cdot min^{-1} \cdot m^{-2}$. E(t) is the fractional extraction of the block, which is zero for the heart-lung and gut blocks.

The insulin influx u(t) to the heart-lung block is the insulin flux in the vena cava, $\varphi_v(t)$:

$$u_{HL}(t) = \varphi_v(t).$$

The insulin influxes to the GUT and OO blocks depend on the aortic flux, $\varphi_a(t)$, and on the fraction of total cardiac output represented by the flow into these organs:

$$u_{GUT}(t) = \frac{F_{pv}}{F}\varphi_a(t),$$

$$u_{OO}(t) = \frac{F_{oo}}{F}\varphi_a(t).$$

The insulin influx to the liver is the sum of the portal vein flux, $\varphi_{pv}(t)$, and the flux in the hepatic artery:

$$u_{LI}(t) = \frac{F_{ha}}{F}\varphi_a(t) + \varphi_{pv}(t),$$

where the portal vein flux is the sum of the gut outflux, $y_{GUT}(t)$, and insulin secretion, ISR(t):

$$\varphi_{pv}(t) = y_{GUT}(t) + ISR(t),$$

The aortic flux is the outflux of the heart-lung block, and the vena cava flux is the sum of the peripheral exogenous insulin infusion, inf(t), and of the outflux of the LI and OO blocks:

$$\varphi_a(t) = y_{HL}(t),$$

$$\varphi_v(t) = y_{OO}(t) + y_{LI}(t) + inf(t).$$

Insulin concentration in the arteries, ins(t), and at the liver inlet, $ins_h(t)$, both expressed as pmol/L, are calculated from the equation of convective flow:

$$ins(t) = \frac{\varphi_a(t)}{F}$$

$$ins_h(t) = \frac{F_{ha}F^{-1}\varphi_a(t) + \varphi_{pv}(t)}{F_{li}}.$$

The initial conditions of all states were set to zero. A time frame lasting 120 min was included before the start of the test simulation via the circulatory model (time zero), with null insulin infusion and ISR(t) equal to the fasting insulin secretion rate from the specific test. This time frame allowed all the model variables to reach steady state levels before time zero.

In the tests stimulating insulin secretion (the hyperglycemic clamp from HGclamp/EUclamp, and the tests from the 3HGclamp, HGclamp, IIGI-OGTT, IIGI-MMTT and RAMP studies), ISR(t) was computed via C-peptide deconvolution using the Van Cauter's model of C-peptide kinetics (12). In

the euglycemic and isoglycemic clamps (from the HGclamp/EUclamp, 2ISOclamp, 2EUclamp and EUclamp studies), ISR(t) was modeled as a function of time, whose estimation was aided by the C-peptide data when available, as detailed below.

Mathematical model of hepatic insulin fractional extraction and clearance.

To account in part for the distributed extraction of insulin in the liver capillary bed, the representation of $E_h(t)$ was inspired to the "tube" capillary model (16,17), in which at steady state plasma insulin concentration at the liver outlet, $ins_{out}(t)$, and inlet, $ins_h(t)$, are related as follows:

$$ins_{out}(t) = ins_h(t) \cdot exp\left(-\frac{cl_{int}}{F_{li}}\right),$$

where cl_{int} is the hepatic intrinsic insulin clearance, quantifying the ability of the hepatic cells, which are exposed to different concentrations along the arteriovenous gradient, to clear insulin independently of the role of blood flow. Hepatic insulin fractional extraction is thus:

$$E_h(t) = 1 - exp\left(-\frac{cl_{int}}{F_{li}}\right).$$

In our representation, we apply these equations to our condition of saturable removal, in which cl_{int} is dependent on insulin concentration and varies with time, $cl_{int}(t)$. We expressed $cl_{int}(t)$ as the ratio of a removal flux, $\gamma(t)$, and insulin concentration at the hepatic inlet, $ins_h(t)$:

$$cl_{int}(t) = \frac{\gamma(ins_h(t))}{ins_h(t)}$$

This equation represents an approximation of the actual "tube" capillary model, in which $cl_{int}(t)$ would be dependent on insulin concentration along the tube. The approximation however retains the concept that the dependence of insulin removal on insulin concentration at cellular level along the capillary is not proportionally reflected in $E_h(t)$, as it is influenced by insulin concentration gradients, which in the liver are remarkable.

The insulin removal flux was modeled using a saturative function of $ins_h(t)$:

$$\gamma(ins_h) = \sigma \cdot ins_h - \sigma \cdot \frac{\frac{log\left(cosh\left(p_1 \cdot (ins_h - p_2)\right)\right) - log(cosh(p_1 \cdot p_2))}{p_1} + tanh(p_1 \cdot p_2) \cdot ins_h}{1 + tanh(p_1 \cdot p_2)}.$$

This function has the following properties: 1) $\gamma(0) = 0$ and $\gamma(ins_h) > 0$ for $ins_h > 0$; 2) $\gamma(ins_h)$ is quasi-linear for ins_h below a threshold represented by p_2 and asymptotically constant above; 3) p_2 is the insulin level around which the slope of $\gamma(ins_h)$ changes from the initial value σ to the final zero value; 4) p_1 determines the curvature of the function around the threshold insulin level p_2 (brisk and gradual transitions are described by high and low p_1 values, respectively). The shape of $\gamma(ins_h)$ was thus determined by three parameters: the initial slope (σ), the threshold insulin level (p_2), and a parameter determining the smoothness of the slope change (p_1).

Whole-organ hepatic insulin clearance, $CL_h(t)$, was calculated as the product $F_{li} \cdot E_h(t)$, and hepatic removal as $CL_h(t) \cdot ins_h(t)$.

Computation of insulin secretion rate in the euglycemic and isoglycemic clamps.

The time course of ISR could not be accurately determined via C-peptide deconvolution during the euglycemic and isoglycemic clamps (from the HGclamp/EUclamp, 2ISOclamp, 2EUclamp and EUclamp studies), as C-peptide concentration was not measured during these tests or was available only at sparse time points. In these studies, ISR was assumed to change gradually from baseline according to the following function:

$$ISR(t) = ISR_0 \cdot (f_{ISR} + (1 - f_{ISR}) \cdot exp\left(-\frac{t}{\tau_{ISR}}\right)),$$

where t is the time after the start of the clamp insulin infusion, ISR_0 is baseline ISR (i.e. ISR at $t \leq 0$), τ_{ISR} is the time constant modulating the speed of change, and f_{ISR} is a positive number describing the relative asymptotic change of ISR(t) (i.e., ISR(t) tends to $ISR_0 \cdot f_{ISR}$ as t tends to infinity). To ensure that ISR(t) reaches a steady state during the final period of the clamp (i.e., since 80 min), the value for τ_{ISR} was constrained to be less than 17.37 min. This is the time constant producing a 99% change in an exponential function at t = 80 min, the minimum time for which steady-state C-peptide data were available in some clamps.

Accounting for insulin and C-peptide assay heterogeneity.

In order to account for potential differences in the insulin and C-peptide assays used in the various studies, correction factors were used. In particular, C-peptide concentration was multiplied by f_{cp}, and

insulin concentration by f_{ins}. These factors differed in the various studies. The EUclamp study was taken as the reference and its f_{ins} value was fixed to one. f_{cp} was fixed to one in the 2ISOclamp study as well, as C-peptide was not measured in this case.

Distributions of individual parameters.

The model parameters were described according to the mixed-effect approach. Inter-individual parameter variability was assumed for most parameters and described by means of specific probability distributions: lognormal for σ, p_1, p_2, ISR_0, and f_{ISR}, logit-normal between zero and one for E_{eh}, logit-normal between 0 and 17.3718 for τ_{ISR}. The individual values of σ and p_2 were assumed to be correlated. Null inter-individual variability and positivity were assumed for the values of f_{cp} and f_{ins} in the different studies. Lognormal inter-occasion variability (besides inter-individual variability) was assumed for ISR_0 in the HGclamp/EUclamp study, in order to estimate different but correlated values for ISR_0 in the two clamps of the same subject. No inter-occasion variability was assumed for the other model parameters.

Parameters estimation.

The estimation procedure was performed by fitting the model predictions to the insulin data from all tests and subjects. In the 2EUclamp and EUclamp studies, C-peptide data were fitted simultaneously: the time course of C-peptide concentration in each test was modelled as the ratio between the modelled ISR(t) and Van Cauter's estimate of C-peptide clearance (12). In the 2ISO clamp study no C-peptide data were available. In the hyperglycemic clamps of the HGclamp/EUclamp study, ISR(t) was determined via C-peptide deconvolution (as in all studies stimulating insulin secretion), while in the euglycemic clamps of the same study no C-peptide data were available. However, baseline C-peptide data from the hyperglycemic clamps and from the OGTT's in the same individuals were fitted to estimate the inter-occasion variability of ISR_0 and the individual values of ISR_0 in the three tests of the HGclamp/EUclamp study: the individual values of ISR_0 in the euglycemic clamps were used in the definition of the time course of ISR (equation above).

The individual parameter estimates were determined in two steps: the means and standard deviations of the normally transformed distributions and the parameters without inter-individual variability were estimated first, and the derived distributions were then used as priors to estimate the maximum-a-posteriori individual-specific (and occasion-specific) values of the parameters. Back transformation of the means of the normally transformed distributions provided the estimates of the population medians, called "typical values" of the parameters. Parameter estimation was performed with the Monolix software, version 4.3.2 (18), which estimates the distributions in the first step via the Stochastic Approximation of Expectation Maximization (SAEM) algorithm, with the Simulated Annealing option.

A key feature of the mixed-effect approach (a.k.a. population approach) is the assumption of a probability distribution for some of the estimated parameters in the population. Thus, if in a subject the data do not allow precise parameter estimation, i.e., very different values could be compatible with the data, the method choses values that are aligned with the probability distribution. Importantly, this occurs preserving the accuracy of the data fit, as shown in Figure S1.

The estimated typical values for the study-independent parameters, together with their inter-individual (and inter-occasion) variability, are provided in Table S8. Values of f_{cp} and f_{ins} estimated in the different studies were between 0.82 and 1.23. The parameter values which were fixed, i.e. not estimated, were the values of t_M in the HL, GUT, LI and OO blocks, and those shown in Table S7.

Model development process.

The mathematical model presented here is the result of a complex model development process, aimed at investigating possible alternatives in its structural and stochastic components. The different steps of the process were guided by physiological plausibility of the equations, parsimony in the number of parameters to be estimated, and increase of the likelihood function, which measures the accuracy of the data fit against the variability in the random components of the model. In particular, we investigated different mathematical descriptions of E_h and E_{eh}, different correlation structures for the

individual values of the model parameters, and the addition of inter-individual variability in cardiac output.

Role of model assumptions.

The use of EIC, rather than hepatic and extrahepatic clearance, was motivated by its relative insensitivity to the assumptions of the mathematical model of insulin kinetics. In fact, EIC and its dependence on insulin secretion could be determined experimentally by means of a stepped hyperglycemic clamp, as the ratio of insulin secretion rate, calculated by C-peptide deconvolution, and peripheral insulin concentration, during the steady-state periods of the clamp. If a mathematical model is used to fit data from such a test to calculate EIC, as long as the model fit is adequate, the model necessarily predicts the ratio of insulin secretion to insulin concentration correctly. Thus, in this case the model assumptions are irrelevant. Even if the model prediction of hepatic and extrahepatic clearance were inaccurate (e.g., because the assumption of constant extrahepatic clearance is not fulfilled), EIC would not be affected.

The assumptions concerning organ blood flows and volumes have little impact on EIC. At steady state, clearance is in fact flow-independent. The organ volumes, which determine the organ transit time density functions, become relevant only in nonsteady-state conditions (13,14). Our experimental tests were mostly in quasi-steady state conditions (although the model predicted correctly also the rapid changes during first-phase or post-arginine insulin secretion).

For similar reasons, the assumptions for the hepatic clearance model are relevant as long as they allow a prediction of EIC consistent with the experimental data, i.e., they allow accurate data fitting. The use of principles derived from capillary bed models (in a formulation that does not require additional parameters), but without an explicit representation of the capillary bed (which would require partial differential equations and considerably more assumptions and parameters), was a way to increase the likelihood of a satisfactory representation of the dependence of EIC on portal insulin concentration. As for the other organs, the approximate representation of the liver insulin dynamics has little relevance in quasi-steady-state conditions.

Probably the most influential aspect for EIC estimation is the availability of appropriate data. As outlined above, a stepped hyperglycemic clamp spanning a wide insulin range would allow model-independent estimation of EIC, while the information provided by a single-dose euglycemic hyperinsulinemic clamp is limited. For this reason, we exploited multiple datasets in conjunction with a mixed-effect modeling approach, as a way to interpret a variety of experiential data informative on EIC with a consistent model. The greater relevance of the model representation of EIC with the less informative experimental protocols was offset by the inclusion of a large number of subjects sharing a unique multivariate probability distribution and undergoing various experimental conditions.

A glucose homeostasis simulator to assess the impact on glucose homeostasis of insulin clearance modulation by ISR

A simplified glucose homeostasis simulator was developed on the basis of a previous prototypical simulator (19). The simulator assembles a model of glucose kinetics (19), a model of insulin secretion (20) and the model of insulin kinetics described herein (Figure S8, left panel). The insulin kinetics model does not consider that insulin clearance reduction was found to be slightly enhanced after glucose or mixed meal ingestion (see *Insulin kinetics after glucose ingestion* in the Results section of the main text). In the original model of insulin secretion (20), potentiation is a time-dependent function that cannot be predicted from glucose. Therefore, in the simulations described below we used a simplified representation with no potentiation effects (i.e. potentiation equal to one).

The parameter values for the glucose kinetics model were set to the estimated typical values published by Bizzotto et al. (19). The β-cell model parameters were chosen as the mean values reported by Mari et al. (20) for healthy subjects: β-cell glucose sensitivity = 148 $pmol \cdot min^{-1} \cdot m^{-2} \cdot mM^{-1}$; rate sensitivity = 908 $pmol \cdot m^{-2} \cdot mM^{-1}$; secretion at 5 mmol/L glucose for the OGTT simulation = 136 $pmol \cdot min^{-1} \cdot m^{-2}$. The insulin kinetics parameters were set to the estimated typical values presented with this work (Table S8).

Impact on glucose homeostasis of insulin clearance modulation by ISR.

The homeostasis simulator was used to assess the impact on an OGTT of insulin clearance being dependent on ISR (as described in this work) or independent on it (as in several published mathematical models of insulin kinetics and glucose homeostasis). To evaluate the effects of insulin clearance modulation, two simulations were performed: one with the full insulin kinetics model, which includes saturative liver insulin extraction, and one in which insulin clearance was kept constant throughout the OGTT, and equal to its fasting value. In both simulations, the model was used to predict insulin and glucose concentrations during an OGTT.

Fasting glucose concentration was fixed to 5 mmol/L. The glucose rate of appearance, Ra(t), was computed before the test as the value producing the assumed basal glucose concentration, and afterwards as the sum of this value and the mean change from baseline of the glucose rate of appearance in eight non-diabetic volunteers from the EUclamp study (19).

The reduction in insulin clearance due to increased ISR after an OGTT, compared with insulin clearance kept at its fasting value, produced remarkable effects on both insulin and glucose time courses (Supplemental Figure S8, right panel): mean arterial insulin concentration increased from 340 to 401 pmol/L, with its a peak raising from 459 to 719 pmol/L; mean glucose concentration decreased from 8.9 to 8.5 mmol/L, and 2-h glucose from 7.0 to 5.5 mmol/L. These effects do not take into account the strengthened reduction of oral *vs* intravenous insulin clearance with hypersecretion (as shown in the previous paragraph): if this were considered, the estimated impact on glucose homeostasis would be even stronger.

Figure 3, panel B: selection of insulin sensitive and resistant subjects, and of reference ISR values

We selected, for M/I, two ranges of values, based on percentiles among non-diabetic subjects (p_k is the kth percentile of M/I): the range p_{85}-p_{95}, representing insulin sensitive (IS) subjects and the range p_5-p_{15}, representing insulin resistant (IR) subjects. The IS M/I range was 194.1-250.8 $\mu mol \cdot min^{-1} \cdot kg^{-}$

^{1}·nmol^{-1}·L, computed per kg of fat-free mass (color blue in the figure), while the IR range was 27.3-49.8 μmol·min^{-1}·kg^{-1}·nmol^{-1}·L (red, light blue, and purple lines in the figure).

For ISR, we used reference values of 50 and 120 pmol·min^{-1}·m^{-2}. These two values correspond to the average fasting ISR values in the two M/I subject subgroups described above: the IS subgroup had fasting ISR of 55±16 (mean±SD), the IR subgroup had fasting ISR of 125±48 pmol·min^{-1}·m^{-2}.

References

1. Toschi E, Camastra S, Sironi AM, Masoni A, Gastaldelli A, Mari A, et al. Effect of acute hyperglycemia on insulin secretion in humans. Diabetes. 2002;51(suppl 1):S130–3.

2. DeFronzo RA, Tobin JD, Andres R. Glucose clamp technique: a method for quantifying insulin secretion and resistance. Am J Physiol. 1979 Sep;237(3):E214-223.

3. Natali A, Ribeiro R, Baldi S, Tulipani A, Rossi M, Venturi E, et al. Systemic inhibition of nitric oxide synthesis in non-diabetic individuals produces a significant deterioration in glucose tolerance by increasing insulin clearance and inhibiting insulin secretion. Diabetologia. 2013 May 1;56(5):1183–91.

4. Seghieri M, Rebelos E, Astiarraga BD, Baldi S, Mari A, Ferrannini E. Impact of a mild decrease in fasting plasma glucose on β-cell function in healthy subjects and patients with type 2 diabetes. Am J Physiol Endocrinol Metab. 2016 01;310(11):E919-924.

5. Muscelli E, Mari A, Casolaro A, Camastra S, Seghieri G, Gastaldelli A, et al. Separate Impact of Obesity and Glucose Tolerance on the Incretin Effect in Normal Subjects and Type 2 Diabetic Patients. Diabetes. 2008 May 1;57(5):1340–8.

6. Muscelli E, Casolaro A, Gastaldelli A, Mari A, Seghieri G, Astiarraga B, et al. Mechanisms for the antihyperglycemic effect of sitagliptin in patients with type 2 diabetes. J Clin Endocrinol Metab. 2012 Aug;97(8):2818–26.

7. Natali A, Gastaldelli A, Camastra S, Sironi AM, Toschi E, Masoni A, et al. Dose-response characteristics of insulin action on glucose metabolism: a non-steady-state approach. Am J Physiol-Endocrinol Metab. 2000;278(5):E794–801.

8. Ferrannini E, Gastaldelli A, Miyazaki Y, Matsuda M, Mari A, DeFronzo RA. beta-Cell Function in Subjects Spanning the Range from Normal Glucose Tolerance to Overt Diabetes: A New Analysis. J Clin Endocrinol Metab. 2005 Jan;90(1):493–500.

9. Ferrannini E, Balkau B, Coppack SW, Dekker JM, Mari A, Nolan J, et al. Insulin resistance, insulin response, and obesity as indicators of metabolic risk. J Clin Endocrinol Metab. 2007 Aug;92(8):2885–92.

10. Arslanian S, Kim JY, Nasr A, Bacha F, Tfayli H, Lee S, et al. Insulin sensitivity across the lifespan from obese adolescents to obese adults with impaired glucose tolerance: Who is worse off? Pediatr Diabetes. 2018;19(2):205–11.

11. Michaliszyn SF, Mari A, Lee S, Bacha F, Tfayli H, Farchoukh L, et al. beta-Cell Function, Incretin Effect, and Incretin Hormones in Obese Youth Along the Span of Glucose Tolerance From Normal to Prediabetes to Type 2 Diabetes. Diabetes. 2014 Nov;63(11):3846–55.

12. Van Cauter E, Mestrez F, Sturis J, Polonsky KS. Estimation of Insulin Secretion Rates from C-Peptide Levels. Comparison of Individual and Standard Kinetic Parameters for C-Peptide Clearance. Diabetes. 1992 Jan 3;41(3):368–77.

13. Mari A. Circulatory Models of Intact-body Kinetics and their Relationship with Compartmental and Non-compartmental Analysis. J Theor Biol. 1993 Feb 21;160(4):509–31.

14. Mari A. Calculation of organ and whole-body uptake and production with the impulse response approach. J Theor Biol. 1995 Jun 7;174(3):341–53.

15. Valentin J. Basic anatomical and physiological data for use in radiological protection: reference values: ICRP Publication 89: Approved by the Commission in September 2001. Ann ICRP. 2002 Sep;32(3–4):1–277.

16. Lassen NA, Perl W. Tracer kinetic methods in medical physiology. New York: Raven Press; 1979. 189 p.

17. Winkler K, Bass L, Keiding S, Tygstrup N. The effect of hepatic perfusion on assessment of kinetic constants. In: Alfred Benson Symposium VI. Munksgaard Copenhagen; 1974. p. 797–807.

18. Lixoft. MONOLIX [Internet]. 2016. Available from: http://lixoft.com/products/monolix/

19. Bizzotto R, Natali A, Amalia Gastaldelli, Elza Muscelli, Martin Krssak, Brehm A, et al. Glucose uptake saturation explains glucose kinetics profiles measured by different tests. Am J Physiol Endocrinol Metab. 2016 Aug 1;311(2):E346-357.

20. Mari A, Tura A, Gastaldelli A, Ferrannini E. Assessing insulin secretion by modeling in multiple-meal tests. Diabetes. 2002;51(suppl 1):S221–6.

21. Goresky CA. A linear method for determining liver sinusoidal and extravascular volumes. Am J Physiol. 1963 Apr;204(4):626–40.

22. Tura A, Pacini G, Kautzky-Willer A, Gastaldelli A, DeFronzo RA, Ferrannini E, et al. Estimation of prehepatic insulin secretion: comparison between standardized C-peptide and insulin kinetic models. Metabolism. 2012 Mar;61(3):434–43.

Table S1. Standardized coefficients and *p* values (as superscripts) in the multivariate linear regression model of EIC_{100} in the EUclamp and HGclamp/EUclamp studies, before and after removal of one independent variable.

IV (rows) \ Removed IV (columns)[a]	M/I	race (AA)	Gm	sex (female)	fISR5	age:female	GS
M/I	**0.56*****	0.57***	0.49***	0.54***	0.52***	0.56***	0.55***
race (AA)	-0.56***	**-0.36****	-0.42***	-0.36**	-0.39***	-0.38***	-0.37**
Gm	$-0.04^{0.04}$	0.15***	**0.14*****	0.14***	0.12***	0.13***	0.11***
sex (female)	$0.02^{0.52}$	-0.13***	-0.14***	**-0.14*****	-0.10*	-0.14***	-0.13***
fISR5	$0.01^{0.52}$	0.12***	0.09***	0.10***	**0.11*****	0.12***	0.12***
age:female	$-0.04^{0.17}$	-0.09**	$-0.06^{0.02}$	-0.09**	-0.10**	**-0.08****	-0.08*
GS	$0.00^{0.96}$	0.06**	$0.00^{0.94}$	0.05*	0.06**	0.06*	**0.06****

[a] IV: independent variable. The diagonal cells (bold red) show standardized coefficients and *p* values without removal of any independent variable.
M/I: insulin sensitivity; AA: African American; Gm: mean oral glucose tolerance test glucose; fISR5: insulin secretion rate at 5 mmol/L glucose in fasting conditions; GS: β-cell glucose sensitivity; *: $p<0.01$; **: $p<0.001$; ***: $p<0.0001$.

Table S2. Standardized coefficients and *p* values (as superscripts) in the multivariate linear regression model of EIC_{400} in the EUclamp and HGclamp/EUclamp studies, before and after removal of one independent variable.

IV (rows) \ Removed IV (columns)[a]	M/I	sex (female)	fISR5	age:female	Gm	age:M/I	fG	GS
M/I	**0.68*****	0.65***	0.64***	0.67***	0.64***	0.67***	0.68***	0.67***
sex (female)	$0.04^{0.31}$	**-0.16*****	-0.15***	-0.17***	-0.15***	-0.15***	-0.18***	-0.15***
fISR5	$0.01^{0.80}$	0.12***	**0.13*****	0.13***	0.14***	0.13***	0.10***	0.13***
age:female	$-0.07^{0.04}$	-0.12***	-0.13***	**-0.12*****	-0.11**	-0.10**	-0.12***	-0.12***
Gm	-0.11**	0.10**	0.13***	0.10**	**0.11*****	0.11***	0.15***	0.07*
age:M/I	$0.06^{0.03}$	0.08**	0.10***	0.07*	0.09**	**0.09*****	0.10***	0.09**
fG	0.08*	0.09**	$0.00^{0.86}$	0.07*	0.12***	0.08**	**0.07***	0.08**
GS	$-0.01^{0.68}$	$0.05^{0.01}$	0.08**	0.06*	$0.02^{0.26}$	0.06*	0.07**	**0.06***

[a] IV: independent variable. The diagonal cells (bold red) show standardized coefficients and *p* values without removal of any independent variable.
M/I: insulin sensitivity; fISR5: insulin secretion rate at 5 mmol/L glucose in fasting conditions; Gm: mean oral glucose tolerance test glucose; fG: fasting glucose; GS: β-cell glucose sensitivity; *: $p<0.01$; **: $p<0.001$; ***: $p<0.0001$.

Table S3. Standardized coefficients and *p* values (as superscripts) in the multivariate linear regression model of EIC_{red} in the EUclamp and HGclamp/EUclamp studies, before and after removal of one independent variable.

IV (rows) \ Removed IV (columns)[a]	M/I:EUclamp	fG	fISR5
M/I:EUclamp	**-0.50*****	-0.47***	-0.48***
fG	$-0.05^{0.15}$	**-0.12*****	-0.08*
fISR5	$0.03^{0.84}$	$-0.02^{0.46}$	**-0.08***

[a] IV: independent variable. The diagonal cells (bold red) show standardized coefficients and *p* values without removal of any independent variable.
M/I: insulin sensitivity; fG: fasting glucose; fISR5: insulin secretion rate at 5 mmol/L glucose in fasting conditions; *: $p<0.01$; **: $p<0.001$; ***: $p<0.0001$.

Table S4. Standardized coefficients and *p* values (as superscripts) in the multivariate linear regression model of EIC_{100} in the EUclamp and HGclamp/EUclamp studies, considered together or separately.

Study (rows) / Independent variable (columns)	M/I	race (AA)	Gm	sex (female)	fISR5	age:female	GS	adjusted R^2
EUclamp & HGclamp/EUclamp	0.56***	-0.36**	0.14***	-0.14***	0.11***	-0.08**	0.06**	0.68
EUclamp	0.64***	-	0.21***	-0.27***	0.18***	-0.07	0.08*	0.31
HGclamp/EUclamp	0.42***	-0.44*	0.20	0.11	0.09	0.01	0.16	0.20

M/I: insulin sensitivity; AA: African American; Gm: mean oral glucose tolerance test glucose; fISR5: insulin secretion rate at 5 mmol/L glucose in fasting conditions; GS: β-cell glucose sensitivity; *: $p<0.01$; **: $p<0.001$; ***: $p<0.0001$.

Table S5. Standardized coefficients and *p* values (as superscripts) in the multivariate linear regression model of EIC_{400} in the EUclamp and HGclamp/EUclamp studies, considered together or separately.

Study (rows) / Independent variable (columns)	M/I	sex (female)	fISR5	age:female	Gm	age:M/I	fG	GS	adjusted R^2
EUclamp & HGclamp/EUclamp	0.68***	-0.16***	0.13***	-0.12***	0.11***	0.09***	0.07*	0.06*	0.59
EUclamp	0.64***	-0.22***	0.17***	-0.12**	0.14***	0.06*	0.10*	0.06	0.33
HGclamp/EUclamp	0.53***	0.03	0.11	0.15	0.20	0.04	0.14	0.25*	0.21

M/I: insulin sensitivity; fISR5: insulin secretion rate at 5 mmol/L glucose in fasting conditions; Gm: mean oral glucose tolerance test glucose; fG: fasting glucose; GS: β-cell glucose sensitivity; *: $p<0.01$; **: $p<0.001$; ***: $p<0.0001$.

Table S6. Standardized coefficients and *p* values (as superscripts) in the multivariate linear regression model of EIC_{red} in the EUclamp and HGclamp/EUclamp studies, considered together or separately.

Study (rows) / Independent variable (columns)	M/I:EUclamp	fG	fISR5	adjusted R^2
EUclamp & HGclamp/EUclamp	-0.50***	-0.12***	-0.08*	0.11
EUclamp	-0.42***	-0.15***	-0.10*	0.17
HGclamp/EUclamp	-	-0.04	-0.06	0.00

M/I: insulin sensitivity; fG: fasting glucose; fISR5: insulin secretion rate at 5 mmol/L glucose in fasting conditions; *: $p<0.01$; **: $p<0.001$; ***: $p<0.0001$.

Table S7. Flow and volume parameters of the mathematical model of insulin kinetics with fixed values derived from the literature.

Block	Plasma flow[a]	Flow calculation	Reference for flow calculation	Volume of distribution[b]	Volume calculation	Reference for volume calculation
HL	1.792	$F_{hl} = 1.00 \cdot F$	(7)	341.5	$V_{hl} = 0.215 \cdot V_p$	(15)
GUT	0.358	$F_{gut} = 0.20 \cdot F$	(15)	142.9	$V_{gut} = 0.090 \cdot V_p$	(15)
LI	0.466	$F_{li} = 0.26 \cdot F$[c]	(15)	191.7	$V_{li} = (10.09/8.36) \cdot 0.100 \cdot V_p$[d]	(15,21)
OO	1.236	$F_{oo} = F - F_{li}$	(15)	1920.5	$V_{oo} = V_{ins} - (V_{hl} + 0.5 \cdot V_{gut} + V_{li})$[e]	(13,22)

[a] Plasma flow in L/min per m^2 of body surface area.
[b] Block volume of distribution in mL/m^2.
[c] The liver flow is the sum of the portal vein flow (0.20·F) and the hepatic artery flow (0.06·F).
[d] The liver volume of distribution was derived assuming that insulin behaves similarly to albumin and estimating albumin liver volume from liver plasma volume (15) and a fixed factor (10.09/8.36, (21)).
[e] The volume of distribution of the OO block is calculated as the difference between whole-body insulin volume (V_{ins}) and the sum of the volumes of the other blocks. Since the gut and the liver are in series, the sum of the volumes must be corrected accounting for the fractional extractions (13), assumed to be negligible in the gut and 0.5 in the liver.
HL or hl: heart and lungs; GUT or gut: gut; LI or li: liver; OO or oo: other organs.
F: total cardiac output as plasma flow, equal to (1-0.44)·3.2 = 1.792 L/min per m^2, where 0.44 is the hematocrit and 3.2 L/min per m^2 of body surface area is the total cardiac output, as blood flow.
V_p: whole-body plasma volume, equal to 1.588 L/m^2, mean of plasma volumes in males (3.0 L) and females (2.4 L), divided by 1.7 m^2 body surface area (15).
V_{ins}: whole-body insulin volume, equal to 2.53 L/m^2, derived from (22).

Table S8. Main parameter estimates of the mathematical model of insulin kinetics.

Parameter	Typical value[a]	Interquartile range[b]
E_{eh} (unitless)	0.213	0.131-0.326
σ ($L \cdot min^{-1} \cdot m^{-2}$)	0.507	0.370-0.695[c]
p_1 (L/pmol)	0.000536	0.000198-0.00145
p_2 (pmol/L)	394	160-973[c]
ISR_0 ($pmol \cdot min^{-1} \cdot m^{-2}$)	71.9	52.7-98.1[d]
f_{ISR} (unitless)	0.856	0.574-1.28
τ_{ISR} (min)	2.48	1.36-4.29[e]

[a] Estimated median of the probability distribution for the specific model parameter.
[b] The range is computed based on the estimated variance of the inter-individual variability on the specific model parameter.
[c] Correlation of individual values for σ and p_2 was estimated to be -0.368.
[d] The interquartile range for inter-occasion variability is 46.4-111.3.
[e] The variance was fixed.

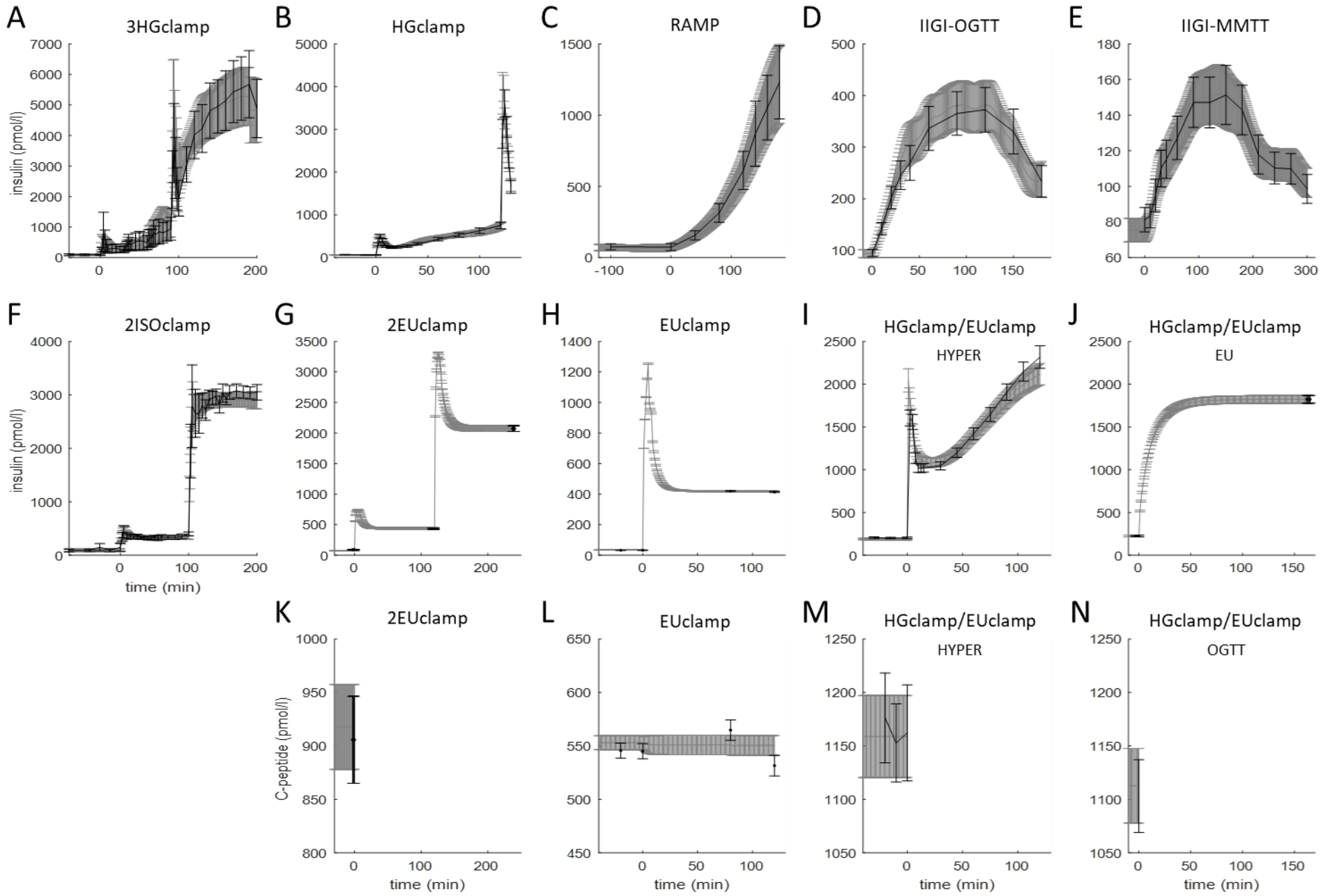
A
3HGclamp
B
HGclamp
C
RAMP
D
IIGI-OGTT
E
IIGI-MMTT
F
2ISOclamp
G
2EUclamp
H
EUclamp
I
HGclamp/EUclamp
HYPER
J
HGclamp/EUclamp
EU
K
2EUclamp
L
EUclamp
M
HGclamp/EUclamp
HYPER
N
HGclamp/EUclamp
OGTT
insulin (pmol/l)
C-peptide (pmol/l)
time (min)

Figure S1. Time course of insulin (panels A-J) and C-peptide (panels K-N) concentration (black) and predictions from the mathematical model of insulin kinetics (grey), as mean±SE. Each panel represents a study, as shown in the panel title. HGclamp/EUclamp study: panel I shows insulin concentration during the hyperglycemic clamp and panel J during the euglycemic clamp; panels M and N show the fit of available C-peptide data, i.e., fasting values from the hyperglycemic clamp and the OGTT, respectively. 2EUclamp study: panels G and K refer to the subject group undergoing insulin infusions of 240 pmol min^{-1} m^{-2} followed by 960 pmol min^{-1} m^{-2}; in this group, fasting C-peptide concentration was available. 2ISOclamp study: only insulin data were available (panel F). HYPER: hyperglycemic clamp; EU: euglycemic clamp.

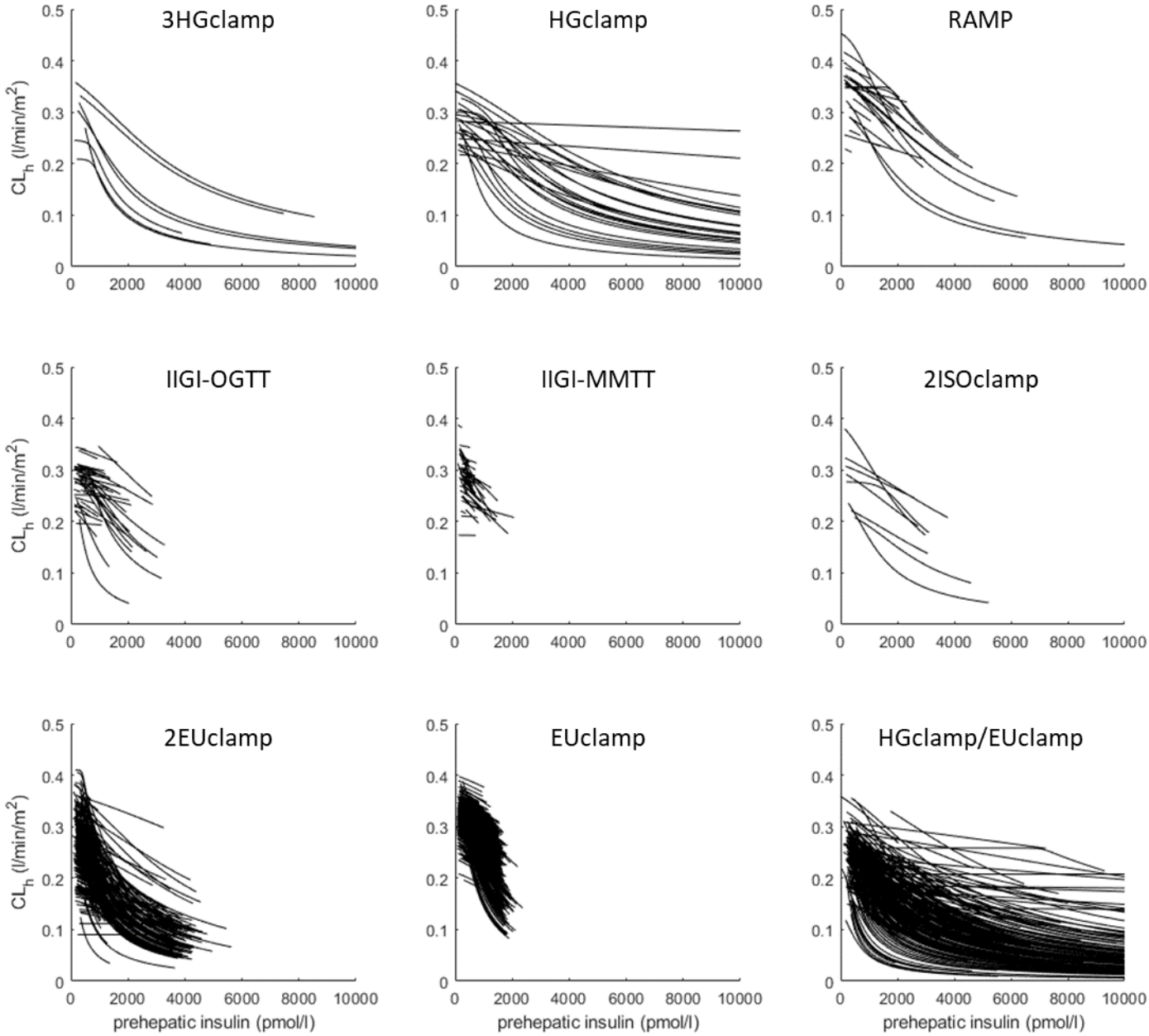

Figure S2. Estimated individual steady-state relationships between prehepatic insulin concentration (x axis) and hepatic clearance (y axis). Each panel represents a specific study, and each curve a specific individual. The hepatic clearance values are shown for the modelled insulin concentration values spanned in each study/individual.

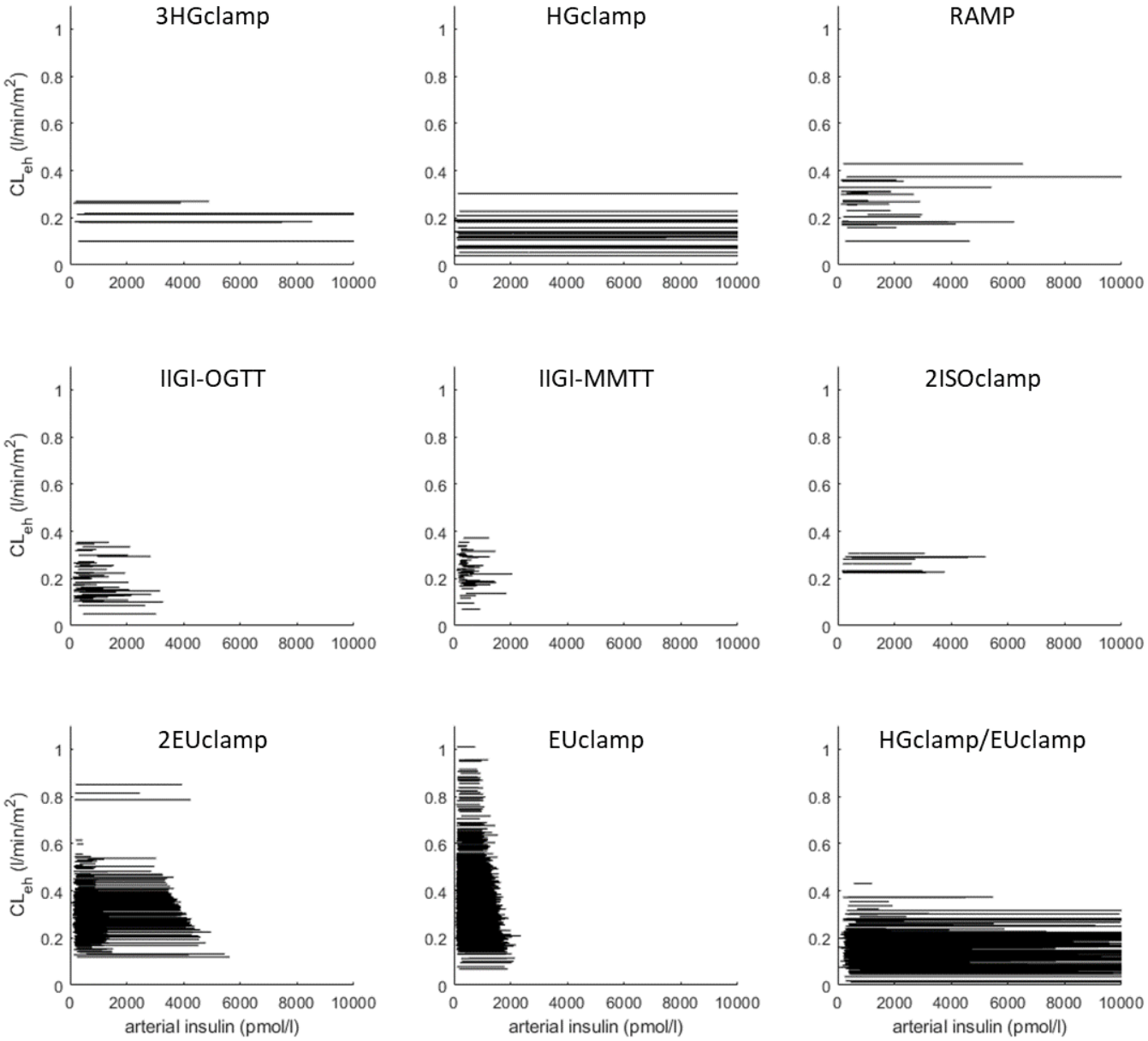

Figure S3. Estimated individual steady-state relationships between arterial insulin concentration (x axis) and extrahepatic clearance (y axis). Each panel represents a specific study, and each curve a specific individual. The extrahepatic clearance values are shown for the modelled insulin concentration values spanned in each study/individual.

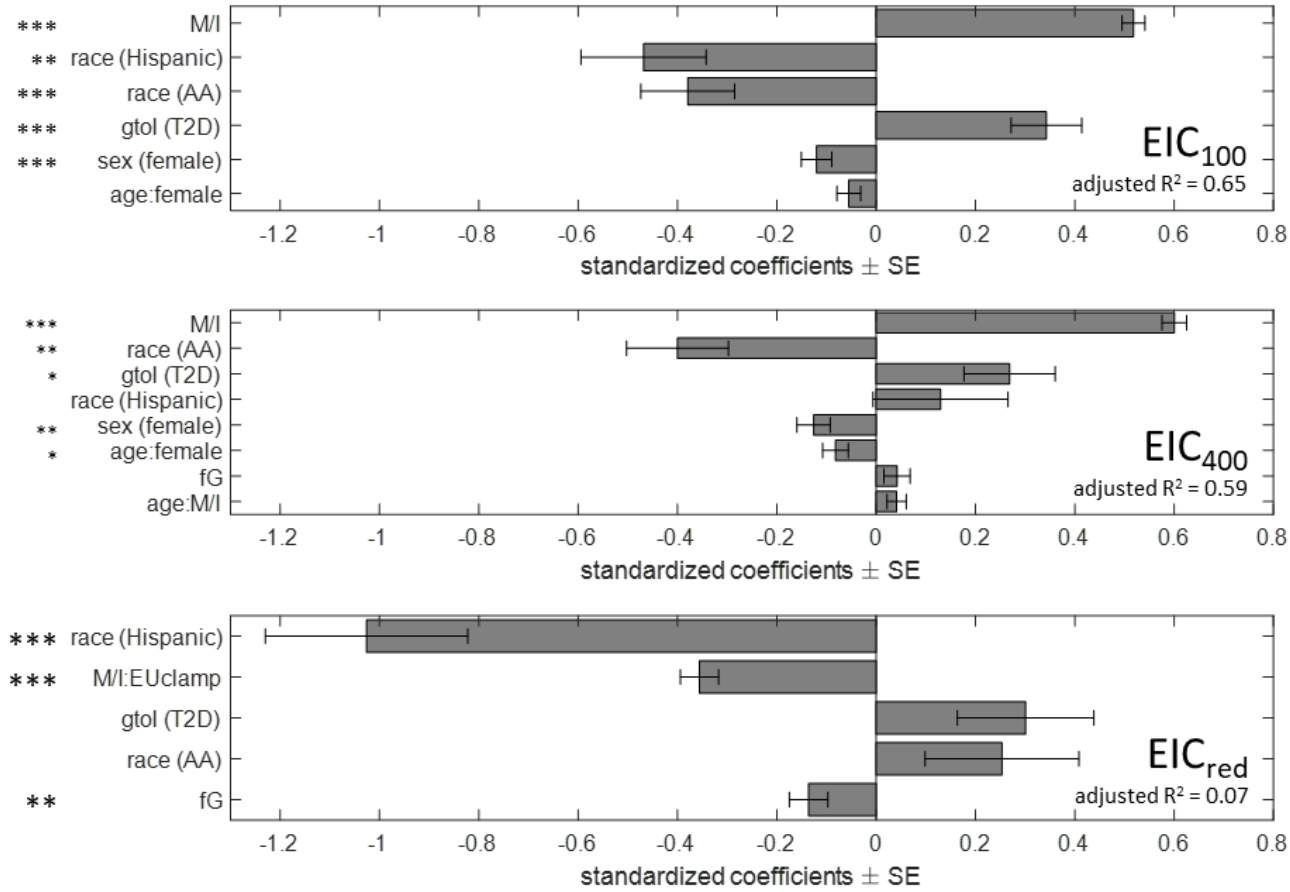

Figure S4. Standardized coefficients from the non-stepwise multivariate linear analyses of EIC_{100}, EIC_{400} and EIC_{red} in the EUclamp, HGclamp/EUclamp, and 2EUclamp studies. The coefficients of the categorical variables are not standardized. M/I, fG, EIC_{100}, and EIC_{400} are log-transformed, EIC_{red} is logit-transformed. M/I: insulin sensitivity; AA: African American; T2D: type 2 diabetes; fG: fasting glucose. *: $p<10^{-2}$; **: $p<10^{-3}$; ***: $p<10^{-4}$.

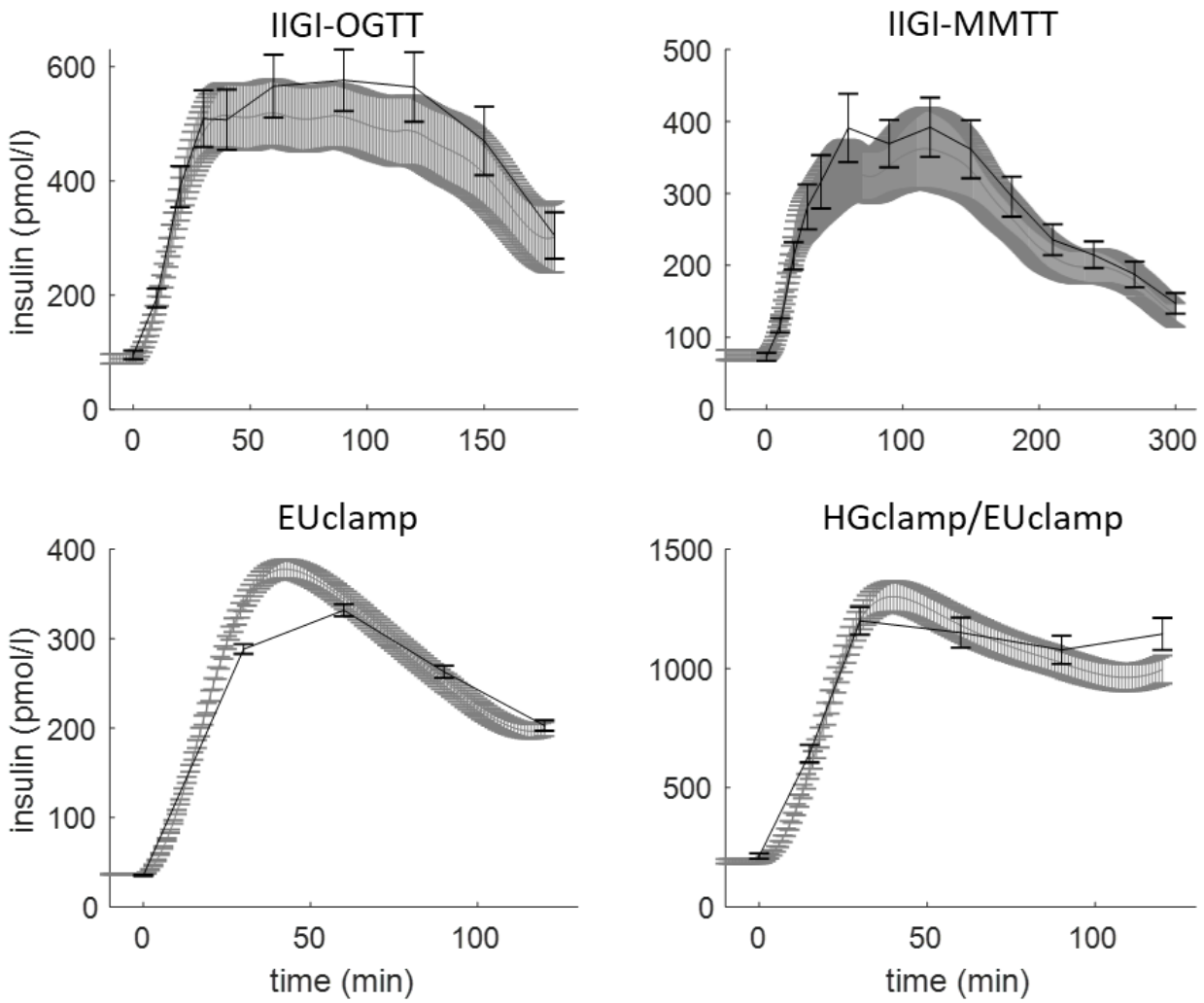

Figure S5. Time course of insulin concentration (black) and predictions from the mathematical model of insulin kinetics (grey) in the studies with oral glucose ingestion, as mean±SE. Each panel represents a specific study (see "Research Design and Methods" section for the names of the studies). The individual predictions are obtained from the mathematical model of insulin kinetics using the individual parameters estimated from the intravenous tests in the same subjects.

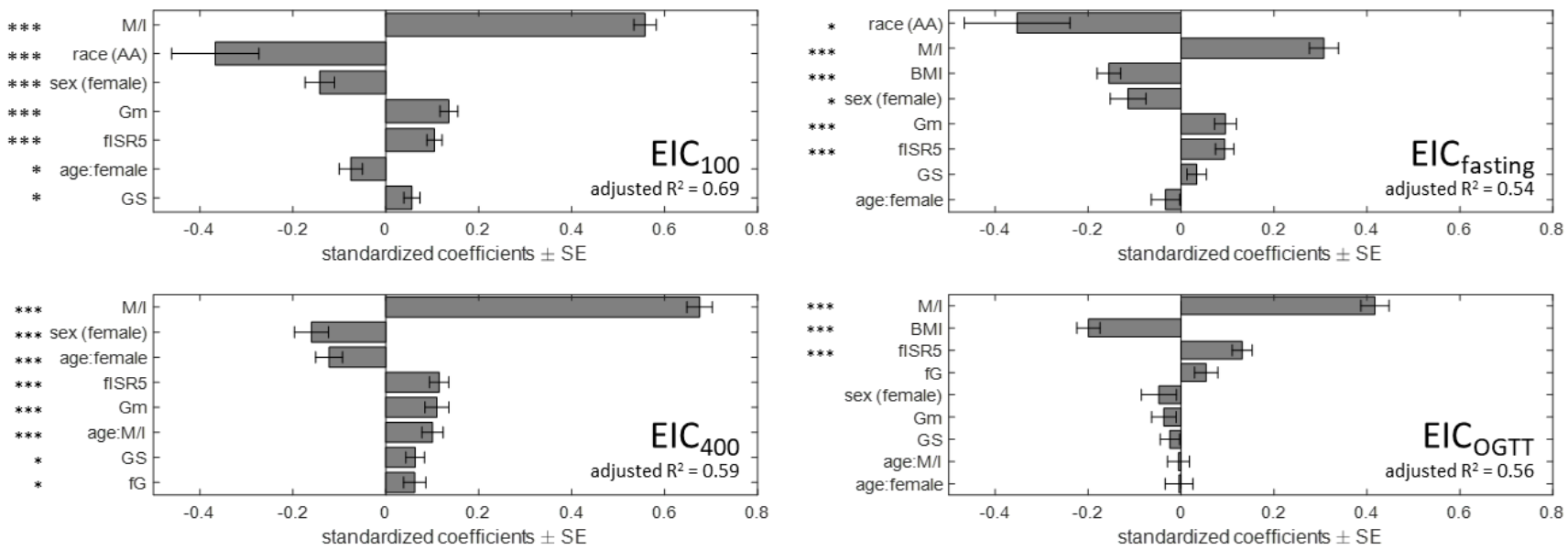

Figure S6. *Left*: standardized coefficients from the multivariate linear analyses of EIC_{100} (top) and EIC_{400} (bottom) in the EUclamp and the HGclamp/EUclamp studies, including the independent variables chosen via stepwise selection (as in Figure 3, Panel A), but only the subjects considered in the right column of this figure (*N*=1380, top, and *N*=1407, bottom). *Right*: standardized coefficients from the multivariate linear analyses of non-standardized EIC in fasting conditions ($EIC_{fasting}$, top panel) and during an OGTT (EIC_{OGTT}, bottom panel), in the EUclamp and the HGclamp/EUclamp studies, including both BMI and the independent variables chosen via stepwise multivariate linear analysis of EIC_{100} and EIC_{400} (see Figure 3, Panel A). $EIC_{fasting}$ is computed as ratio between fasting ISR and insulin concentration; EIC_{OGTT} is computed as ratio between the areas under the curves for ISR and for insulin concentration. In both panels, the coefficients of the categorical variables are not standardized. M/I, BMI, fISR5, fG, EIC_{100}, and EIC_{400} are log-transformed. M/I: insulin sensitivity; AA: African American; Gm: mean oral glucose tolerance test glucose; fISR5: insulin secretion rate at 5 mmol/L glucose in fasting conditions; GS: β-cell glucose sensitivity; fG: fasting glucose. *: $p<10^{-2}$; **: $p<10^{-3}$; ***: $p<10^{-4}$.

A

EUclamp & HGclamp/EUclamp

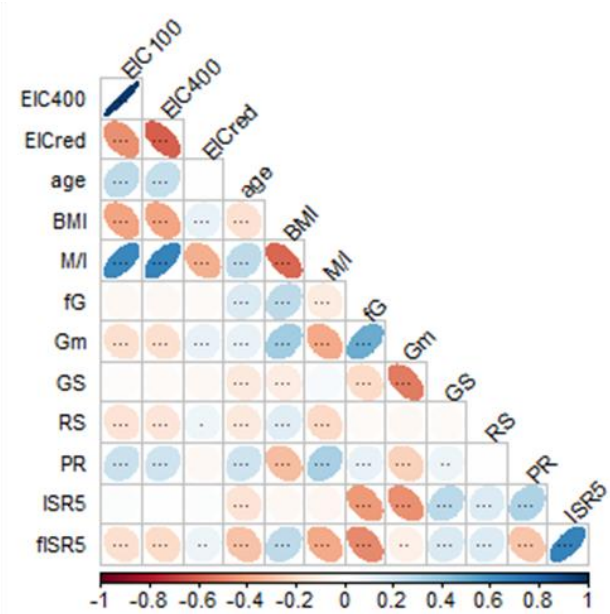

B

EUclamp & HGclamp/Euclamp & 2EUclamp

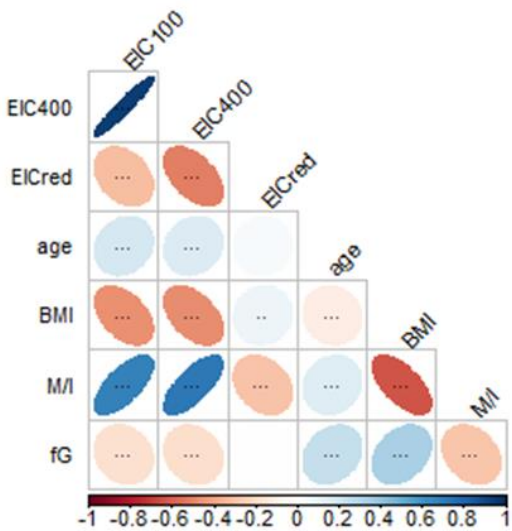

C

Euclamp & HGclamp/EUclamp

Euclamp & HGclamp/Euclamp & 2EUclamp

D

Euclamp & HGclamp/EUclamp

Euclamp & HGclamp/Euclamp & 2EUclamp

E

Euclamp & HGclamp/EUclamp

Euclamp & HGclamp/Euclamp & 2EUclamp

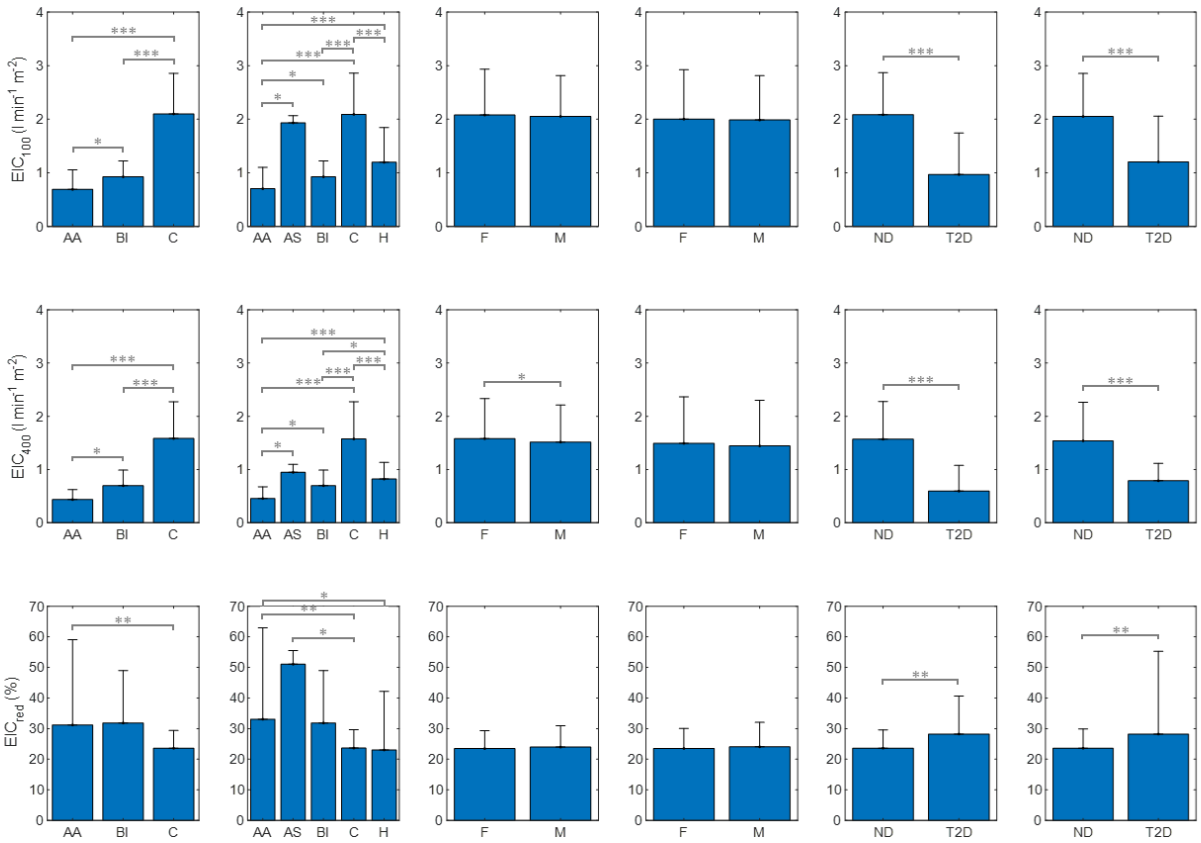

Figure S7. *Panels A, B*: pairwise correlation matrices of the continuous variables considered for the analysis of standardized endogenous insulin clearance in the EUclamp and HGclamp/EUclamp studies (panel A), or in the larger set of EUclamp, HGclamp/EUclamp, and 2EUclamp studies (panel B); fill color represents the sign of the Spearman correlation coefficient (positive in red and negative in blue), and color intensity (see color bars) and the elliptic shape the magnitude. *Panels C, D, E*: median ± interquartile range of EIC_{100}, EIC_{400}, and EIC_{red} according to race (panel C), sex (panel D) and diabetic condition (panel E), computed in the EUclamp and HGclamp/EUclamp studies, or in the larger set of EUclamp, HGclamp/EUclamp, and 2EUclamp studies. Differences are tested via Wilcoxon rank-sum test. Pairwise correlations and differences may not reflect the results of the multivariable regression models presented in the main text. M/I: insulin sensitivity; fG: fasting glucose; Gm: mean oral glucose tolerance test glucose; GS: β-cell glucose sensitivity; RS: rate sensitivity; PR: potentiation factor ratio; ISR5: insulin secretion rate at 5 mmol/L glucose; fISR5: insulin secretion rate at 5 mmol/L glucose in fasting conditions; AA: African American; AS, Asian; BI, biracial African-Caucasian; C, Caucasian; H, Hispanic; F, females; M, males; ND, non-diabetic; T2D: type 2 diabetes. *: $p<0.05$; **: $p<0.01$; ***: $p<0.001$.

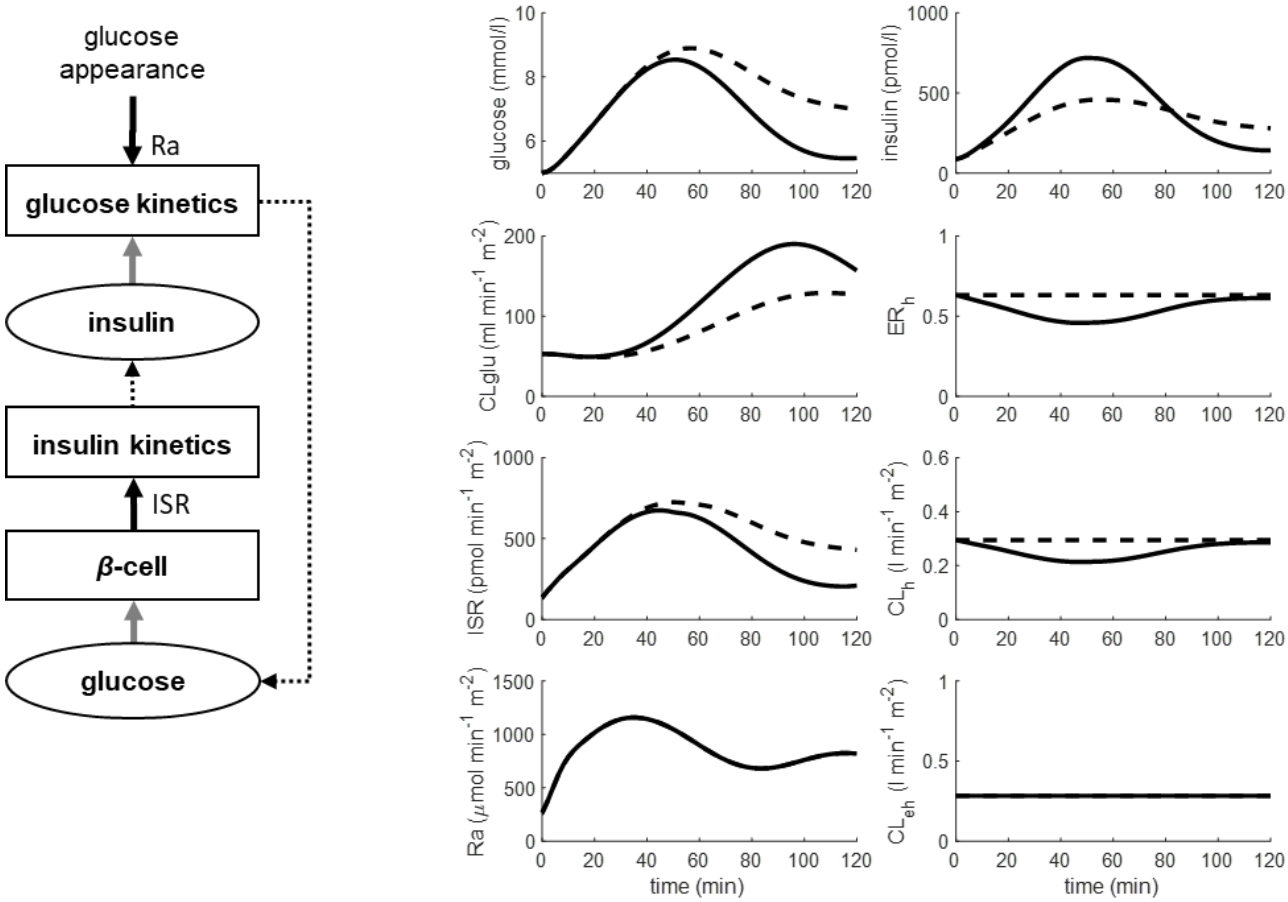

Figure S8. *Left*: schematic representation of the glucose homeostasis simulator, with subsystems depicted with rectangles, mass fluxes depicted with black solid arrows (insulin secretion, ISR, and glucose rate of appearance, Ra), effects depicted with grey solid arrows, and glucose and insulin concentration shown with ellipses and dashed black arrows. *Right*: simulation of the time course of main variables during an OGTT, with insulin clearance depending on insulin levels (solid curve) or kept constant at the fasting level during the whole OGTT (dashed curve). The represented variables are arterial glucose and insulin concentrations, glucose clearance (CLglu), ISR, Ra, hepatic extraction ratio (ER_h), hepatic and extrahepatic insulin clearance (CL_h and CL_{eh}, respectively).

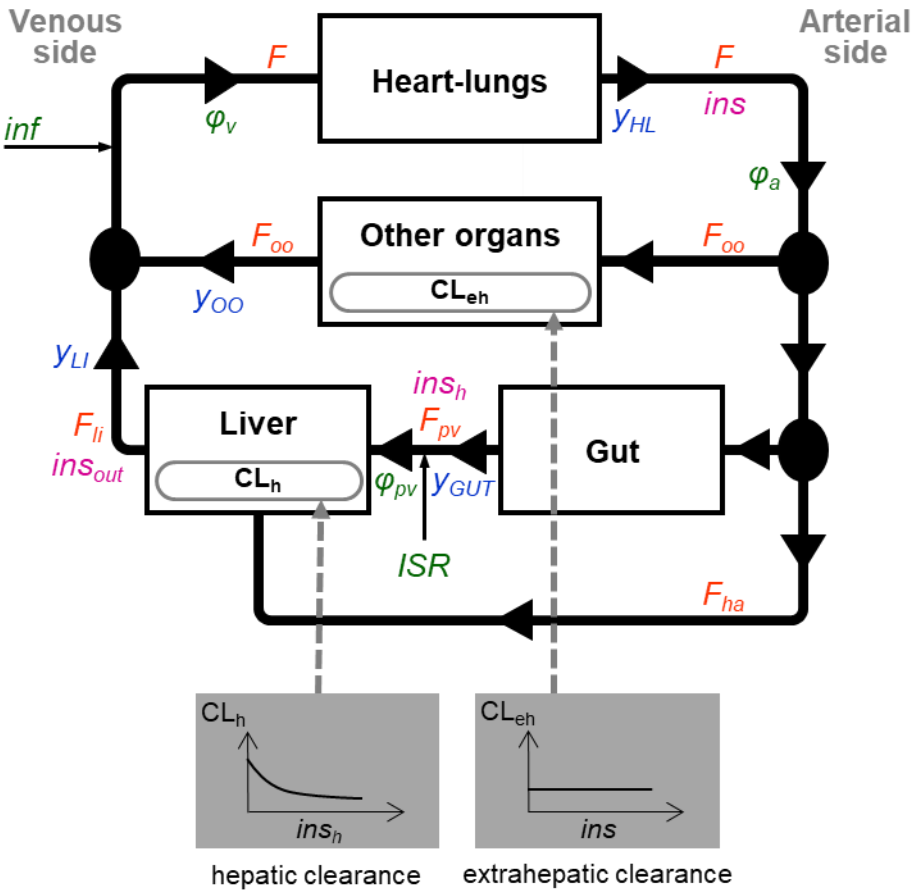

Figure S9. Schematic representation of the mathematical model of insulin kinetics. Compared to Figure 1, this one also includes the symbols used in the detailed model description of the Supplemental Material to indicate plasma flows (in red), insulin mass fluxes (in green), insulin mass outfluxes from specific blocks (in blue), and insulin concentrations (in magenta). As in Figure 1, white rectangles represent lumped organs, black arrows depict fluxes of insulin between the organs, grey rectangles exemplify the relationships between prehepatic insulin concentration and hepatic clearance (left grey rectangle), and between arterial insulin concentration and extrahepatic clearance (right grey rectangle).